Solar Phys (2013) 284:89–104
DOI 10.1007/s11207-013-0242-7

A Comparative Study of Coronal Mass Ejections with and Without Magnetic Cloud Structure near the Earth: Are All Interplanetary CMEs Flux Ropes?

J. Zhang · P. Hess · W. Poomvises

Received: 13 July 2012 / Accepted: 21 January 2013 / Published online: 8 February 2013
© Springer Science+Business Media Dordrecht 2013

Abstract An outstanding question concerning interplanetary coronal mass ejections (ICMEs) is whether all ICMEs have a magnetic flux rope structure. We test this question by studying two different ICMEs, one having a magnetic cloud (MC) showing smooth rotation of magnetic field lines and the other not. The two ICMEs are chosen in such a way that their progenitor CMEs are very similar in remote sensing observations. Both CMEs originated from close to the central meridian directly facing the Earth. Both CMEs were associated with a long-lasting post-eruption loop arcade and appeared as an elliptical halo in coronagraph images, indicating a flux rope origin. We conclude that the difference in the *in-situ* observation is caused by the geometric selection effect, contributed by the deflection of flux ropes in the inner corona and interplanetary space. The first event had its nose pass through the observing spacecraft; thus, the intrinsic flux rope structure of the CME appeared as a magnetic cloud. On the other hand, the second event had the flank of the flux rope intercept the spacecraft, and it thus did not appear as a magnetic cloud. We further argue that a conspicuous long period of weak magnetic field, low plasma temperature, and density in the second event should correspond to the extended leg portion of the embedded magnetic flux rope, thus validating the scenario of the flank-passing. These observations support the idea that all CMEs arriving at the Earth include flux rope drivers.

Flux-Rope Structure of Coronal Mass Ejections
Guest Editors: N. Gopalswamy, T. Nieves-Chinchilla, M. Hidalgo, J. Zhang, and P. Riley

J. Zhang (✉) · P. Hess
School of Physics, Astronomy and Computational Sciences, George Mason University,
4400 University Dr., MSN 6A2, Fairfax, VA 22030, USA
e-mail: jzhang7@gmu.edu

W. Poomvises
Catholic University of America, Washington, DC 20064, USA

W. Poomvises
NASA Goddard Space Flight Center, Greenbelt, MD 20771, USA

1. Introduction

Coronal mass ejections (CMEs) are an energetic phenomenon originated in the Sun's corona, but subsequently propagating into the interplanetary space. CMEs are now well known to be the cause of intense geomagnetic storms (Gosling *et al.*, 1991; Zhang *et al.*, 2007) and to be a direct driver of severe space weather that may have disruptive effects on advanced human technological systems in space and on the ground. The underlying physical structure of a CME is believed to be a magnetic flux rope, a self-contained magnetic system with helical magnetic field lines wrapping around its center axis (Chen, 1996). The first direct observational evidence of the presence of magnetic flux ropes was from near-Earth *in-situ* solar wind observations of the so-called magnetic clouds, seen as a large rotation in the field's direction, enhanced field strength and a low plasma β (Burlaga *et al.*, 1981; Lepping, Jones, and Burlaga, 1990). Improved coronagraphic observations of CMEs from the *Solar and Heliospheric Observatory* (SOHO) showed that CMEs in the outer corona often contain a circular intensity pattern when CMEs are observed from the side, thus suggesting the presence of flux ropes (Dere *et al.*, 1999).

Recent observations from the *Advanced Imaging Assembly* (AIA) on-board *Solar Dynamic Observatory* (SDO) showed that a magnetic flux rope exists prior to the eruption and continuously transforms from a sigmoidal structure to a semi-circular shape (Zhang, Cheng, and Ding, 2012). In SDO observations, magnetic flux ropes are best seen in hot temperature passbands ($> \sim 6$ MK), but are completely absent in cool temperatures ($< \sim 3$ MK) (Liu *et al.*, 2010; Cheng *et al.*, 2011; Zhang, Cheng, and Ding, 2012). Earlier observations of sigmoidal structures in soft X-ray images prior to eruptions (Sterling and Hudson, 1997; Canfield, Hudson, and McKenzie, 1999), are often interpreted as a magnetic flux rope (Rust, 1994; Titov and Démoulin, 1999; McKenzie and Canfield, 2008). The physical origin of flux ropes has been suggested either to be sub-photospheric emergence into the corona (Gibson *et al.*, 2002; Schrijver, 2009), or the transformation of a sheared arcade through photospheric flux cancellation (Green and Kliem, 2009; Tripathi *et al.*, 2009).

Magnetic flux ropes probably play an essential role in CME initiation and acceleration, *i.e.*, the CME initiation is triggered by the structural instability of the flux rope. One such mechanism is so-called the Torus Instability (TI) (Kliem and Török, 2006; Olmedo and Zhang, 2010), an ideal magneto-hydrodynamic (MHD) process responsible for the loss of equilibrium of a toroidal current ring. In this model, a critical gradient of the external magnetic field determines the onset of the instability. Three-dimensional MHD simulations further demonstrate that the transition of a flux rope from equilibrium to eruption follows the TI onset criterion (Fan and Gibson, 2007; Aulanier *et al.*, 2010). However, there also exist opposing models that assume no flux rope prior to the eruption, and assume a sheared arcade instead (Antiochos, DeVore, and Klimchuk, 1999; Moore *et al.*, 2001; Amari *et al.*, 2003). Nevertheless, these models allow magnetic reconnection to transfer the sheared arcade into a fully developed magnetic flux rope. Therefore, on both observational and theoretical grounds, all sizable CMEs following the eruption (*e.g.*, tens of minutes) are likely to contain a magnetic flux rope in the structure.

An interesting and important question is then about the CME structure near the Earth after the tens-of-hour-long journey through the interplanetary space. *In-situ* observations of solar wind magnetic field and plasma properties have clearly revealed the existence of interplanetary CMEs (ICMEs), the counterpart phenomena of CMEs from the Sun. The *in-situ* signatures of ICMEs are many, including enhanced magnetic field, reduced magnetic field variance, abnormally low proton temperature, upstream forward shock, elevated

oxygen charge state, enhancement of Fe/O ratio, and bidirectional strahl electrons *etc.* (Zurbuchen and Richardson, 2006). Not all signatures exist at the same time, but the presence of several signatures set ICMEs apart from the ambient solar wind. One can also set ICMEs apart from other transient features, such as CME-driven sheath regions and corotating interaction regions (CIRs).

It has been found that only a subset of ICMEs show the presence of a magnetic cloud structure or flux rope. These magnetic-cloud ICMEs are abbreviated as MC-ICME hereafter. The complementary set of ICMEs, which do not show a systematic rotation of magnetic field lines, are abbreviated NMC-ICMEs (non-magnetic-cloud ICME). MC-ICMEs only constitute a fraction of all ICMEs detected in solar wind, The estimated fraction ranges from ~ 30 % to ~ 50 % (Gosling, 1990; Bothmer and Schwenn, 1996; Henke *et al.*, 2001). Richardson and Cane (2004) found a solar cycle variation of the fraction of MC-ICMEs, *i.e.*, ~ 15 % at solar maximum but as high as almost 100 % at solar minimum. MC-ICMEs are usually more geoeffective than other transient events. Zhang *et al.* (2007) found that for those ICME-driven intensive geomagnetic storms, 43 % of the storms are caused by MCs, and only 18 % of them are produced by NMC-ICMEs; the others are related to ICME-driven shock sheaths (27 %) and shocks propagating into preceding ICMEs (12 %). Gopalswamy *et al.* (2007) also found that MC-associated CMEs are faster and wider on the average and originate within ± 30 degree from the solar disk center.

The challenging question is whether or not a NMC-ICME is a flux rope, given that there is a large fraction of NMC-ICMEs at 1 AU. We intend to address this issue through a careful comparative study of MC-ICME and NMC-ICME events. If one assumes that all CMEs borne on the Sun are a flux rope, there are several known factors that might cause the flux rope to appear as a non-magnetic-cloud:

i) Geometric selection effect. This effect is caused by the one-point sampling of *in-situ* observations, *i.e.*, the appearance of an ICME is highly dependent on the sampling path of the spacecraft through the ICME structure. This selection effect, as well as the contributing deflection effect of flux ropes, will be addressed in detail in this paper (see the Discussion section).
ii) Multiple CME-interaction effect (Gopalswamy *et al.*, 2001; Wang *et al.*, 2003), in which the interaction possibly destroys the coherence of a flux rope.

We can safely exclude the self-evolution effect of a single flux rope, since it is unlikely that a flux rope topology, while expanding in the interplanetary space, will alter and change itself into some structures different from a flux rope. The interaction between flux rope and the ambient solar wind will possibly compress the flux rope, the so-called pancake effect (Riley and Crooker, 2004), but will not change the overall topology of helical field lines. In this paper, we make a comparative study of two ICMEs, one MC and one NMC. The ICMEs are such chosen so that we remove or limit all the known effects affecting the evolution of flux ropes. Both events are isolated single CMEs, thus eliminating the effect of CME interaction. Both progenitor CMEs originated close to the central meridian of the Sun, thus limiting the difference of initial launching angles. Further, both CMEs were associated with long-lasting post-eruption arcades and elliptic-shaped halo CMEs, suggesting a flux rope origin.

The organization of the paper is as follows. Observations and event selection are given in Section 2, the results of comparative analysis are presented in Section 3, and Section 4 provides discussion and conclusions.

2. Observations and Event Selection

The two events studied in this paper are carefully chosen from a large set of 59 ICME events from 1997 to 2006 whose solar progenitor CMEs and source regions are well defined. These events are the database of two Coordinated Data Analysis Workshops (CDAW), one took place in 2010 and the other in 2011, for the purpose of addressing the question discussed in Section 1. The database of 59 events is available on-line at http://cdaw.gsfc.nasa.gov/meetings/2010_fluxrope/. For each event, the database provides

i) the ICME information, including the arrival time of the shock, the start time and end time of the ICME,
ii) the progenitor CME information near the Sun, including the CME onset time, the width, average velocity and average acceleration, and
iii) CME source region information, including the heliographic coordinates of the source surface region, the associated GOES soft X-ray flare onset time and magnitude.

Among the 59 events, only 25 events can be classified as MC CMEs.

One approach to address the all-flux-rope hypothesis is to make a comparative study of two types of ICME event. A task group in the 2010 workshop was established to select the two types of "well behaved" ICME. The criteria of "well behaved" ICMEs are many, including having low proton temperature, low plasma density, high charge state, expansion velocity profile, enhanced magnetic field, and large scale in duration and size. The only difference between the two types is whether or not the magnetic field shows rotation. Further, the two types are comparable in the properties of progenitor CMEs, *i.e.*, they are all full halo CMEs and comparable in velocities. The properties of their source surface regions are also comparable, in particular, they all originated within 15° of central meridian. After working through the database, the task group down selected the following four events as "well behaved" NMC-ICMEs: 22 September 1999, 22 January 2004, 17 February 2005, and 19 August 2006, which are events numbered as 13, 47, 52, and 59, respectively, in the database. For comparison, the following four events were selected as "well behaved" MC-ICMEs: 11 August 2000, 12 October 2000, 18 May 2002 and 24 July 2004, which are numbered as 23, 26, 39, and 48, respectively, in the database.

In this paper, we choose one event from each type and carry out a detailed analysis on all relevant properties of the events from the Sun to the Earth. The representative MC-ICME occurred on 12 October 2000, while the representative NMC-ICME arrived at the Earth on 22 September 1999.

3. Comparative Analysis and Results

3.1. Properties of the MC Event

The event on 12 October 2000 is a typical MC-ICME. Figure 1 shows the *in-situ* solar wind data obtained from the ACE spacecraft. The time-series data show two distinct periods, one corresponding to the magnetic cloud (the period between two vertical blue lines), and the other corresponding to the shock sheath region (the period between the vertical red line and the vertical solid blue line). The arrival of the event at 1 AU was first signaled by the conspicuous shock at 21:42 UT on 12 October 2000, at which the solar wind velocity, density and temperature as well as the magnetic field showed an abrupt jump in strength. These elevated solar wind parameters continued for about 19 hours, forming the so-called shock

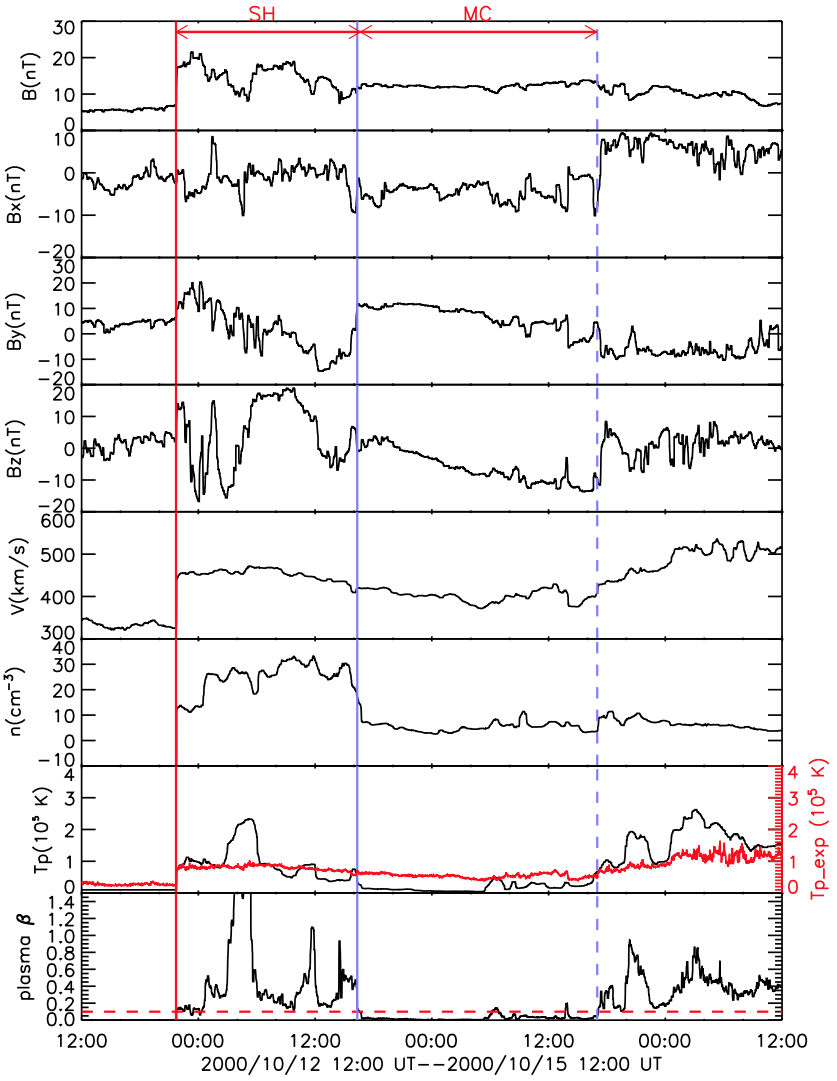

Figure 1 *In-situ* solar wind observations of the ICME event on 12 October 2000. The panels from top to bottom show, respectively, (1) solar wind magnetic field total intensity, (2) magnetic field B_x component, (3) magnetic field B_y component, (4) magnetic field B_z component, (5) solar wind plasma velocity, (6) plasma density, (6) proton temperature (black) overlaid with the expected temperature (red), and (7) the derived plasma β. The solar wind data are from the ACE spacecraft in GSE coordinates. The solid and dashed blue vertical lines indicate the starting and ending times of the ICME, which in this case is a magnetic cloud. The vertical red line indicates the arrival time of the ICME-driven shock.

sheath region. The sheath region ended at 16:20 UT on 13 October 2002, at which time the magnetic cloud, or the CME ejecta started to appear. The onset of the MC was characterized by an abrupt reduction of plasma temperature and density, thus the plasma β, likely caused by the quasi-adiabatic expansion of the magnetic cloud. The magnetic cloud lasted for about 25 hours, ending at about 17:00 UT on 14 October 2000. During the whole period of the magnetic cloud, the magnetic field clearly showed a smooth profile, in contrast to the fluc-

tuating profile in the sheath region. In particular, the magnetic field showed a clear rotation of its vector direction, as evident in the monotonic continuous change of its Z component from the northward maximum to southward maximum. The duration of the magnetic cloud is also well demarcated by the abnormal low temperature, relative to the expected temperature which is empirically determined from the observed solar wind velocity but assuming a normal solar wind condition (as shown in the red line profile in the temperature panel of Figure 1) (Richardson and Cane, 1995).

The solar wind data within the period of the magnetic cloud can be well fitted by the cylinder-shaped force-free flux rope model (Lepping, Jones, and Burlaga, 1990). One can find a catalog of magnetic clouds and their fitting parameters on-line at http://wind.nasa.gov/mfi/clouds/mag_cloud.html. The axis of the fitting flux rope has a direction of latitude $-24°$ (pointing toward the South or negative Z along the Z direction; also called the inclination angle) and longitude 140° (pointing toward the Earth or negative X along the X direction, and toward the East or positive Y along the Y direction; also called the azimuthal angle) in the GSE coordinates. This axial direction will be compared later with the orientations available from various solar observations. The diameter of the flux rope is 0.21 AU, the size of a typical magnetic cloud. The closest approach, defined as the ratio between the spacecraft-axis distance and the radius of the flux rope, is about 17 %.

The orientation of the flux rope determined at 1 AU is largely consistent with the inferred orientations from various remote-sensing observations (Figures 2 and 3). The four panels in Figure 2 shows the progenitor CME (panel d) observed by the LASCO C2 coronagraph, the surface source active region (panel c) observed by the SOHO MDI instrument and the coronal source region by SOHO EIT (panel a and b). The white line in panel b shows the axial orientation of the post-eruption loop arcade associated with the progenitor CME. The accompanying C6.7 GOES X-ray flare located at the heliographic location of N01°W14° is indicated by the plus symbol. This accompanying flare had an onset time at 23:19 UT on 09 October 2000, which should be also the onset time of the CME (Zhang *et al.*, 2001). Thus, it took about 70 hours for the CME-driven shock to reach the Earth, and about 88 hours for the CME ejecta itself to arrive. The latitudinal orientation of the post-eruption loop arcade is found to be 32°, which is about 8° different from the value of 24° of the axial orientation of the magnetic cloud. The difference is rather small, given the uncertainty of the fitting of the magnetic cloud. The orientation of the post-eruption loop arcade aligns well with the polarity inversion line of the magnetic field in the source active region as seen in Figure 2(b). Thus, the orientation of the magnetic cloud is consistent with the orientation of the erupted flux rope inferred from the post-eruption loop arcade and the source region magnetic field.

We can also infer the orientation of the flux rope in the outer corona from coronagraph observations. A halo CME usually has its leading front in all position angles forming an oval shape, as shown by the plus symbols and the fitted elliptical shape in Figure 3. The orientation of the major axis of the fitted ellipse likely indicates the axial orientation of the underlying flux rope. We illustrate this point using the so-called cone model fitting and the difference between the cone-projected ellipse and the observed ellipse. The geometric cone model of CMEs assumes that a CME has an intrinsic cone shape, uniquely determined by the following four parameters: longitude and latitude of the cone axis, angular width, and the height of the cone (Zhao, Plunkett, and Liu, 2002; Xie, Ofman, and Lawrence, 2004). While the cross section of the cone has a perfect circular shape, its projection onto the plane of the sky has usually an elliptic shape when the axis of the cone is not oriented perfectly along the line of sight. We fitted the observed ellipse (the black oval) with the four-parameter cone

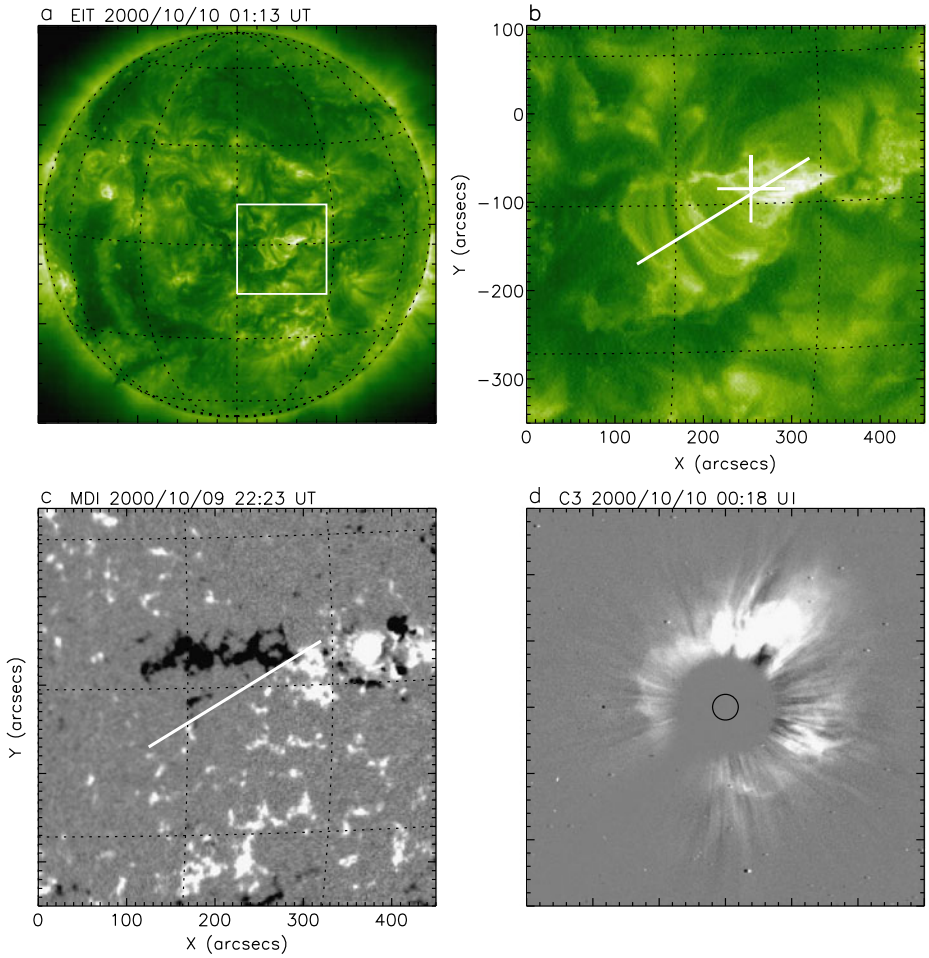

Figure 2 Solar remote-sensing observations of the source region and progenitor CME of the ICME event on 12 October 2000. (a) A full disk SOHO EIT image showing the location of the source region (inside the white square), (b) A zoom-in image of the white square area in panel (a), showing the post-eruption arcade associated with the CME. The white line indicates the orientation of the arcade, while the cross symbol indicates the location of the accompanying flare. (c) A SOHO MDI line-of-sight magnetogram image showing the photospheric magnetic field structure of the CME source region. The white line is the same as in panel (b), indicating that the orientation of the post-eruption arcade follows the polarity inversion line of the magnetic field on the surface. (d) The progenitor halo CME observed by the SOHO LASCO C2 coronagraph.

model, and then projected the cone onto the plane of the sky using the fitting parameters. The result of the cone projection is the ellipse shown in red color in Figure 3. Apparently, the orientation of the major axis of the cone-projected ellipse is much different from that of the observed ellipse; the two major axes are almost orthogonal to each other. We believe that the difference is caused by the shape of the CME, which should be intrinsically an elongated flux rope, instead of a circular cone. The axial orientation of the flux rope gives rise to the major axis of the observed ellipse. It is found that the major axis of the ellipse has a tilt angle of 34°, which is very close to the inferred flux rope orientation based on the post-eruption loop arcade (32°).

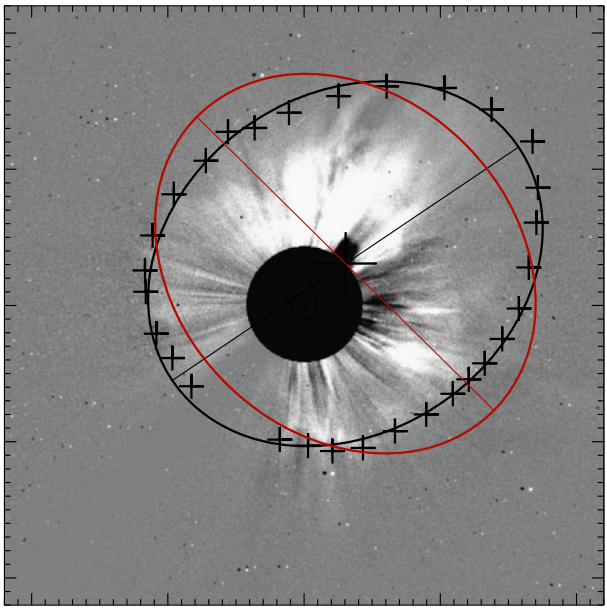

Figure 3 The geometric fitting to the observed progenitor halo CME of the ICME event on 12 October 2000. The black plus symbols are visually selected to outline the edge of the halo CME, which is fitted into an elliptic shape as indicated by the black curve; the straight black line indicates the major axis of the fitted ellipse. The ellipse shape in red line is the expected CME shape assuming a circular cone geometry of the CME, with the red straight line indicating the major axis of the ellipse. Apparently, the observed shape deviates from the circular cone model, indicating a possible flux rope structure of the CME.

We note that it is likely that the elliptical fitting is made on the shock front instead of the CME flux rope itself. In white light coronagraph images, CME-driven shocks usually appear as a diffuse front running ahead of the ejecta, which usually has a sharper contrast in brightness (Vourlidas *et al.*, 2003; Wood and Howard, 2009). Nevertheless, we believe that the elongated shape of the shock front should be similar to that of the flux rope. The flux rope is the underlying driver of the shock, thus any asymmetry in the geometry of the driver will likely to show up in the appearance of the driven front. The shape of the shock may be further deformed if there exists a nearby coronal hole, which allows the shock to propagate faster inside the hole than in surrounding regions (Wood *et al.*, 2012). For the event studied here, the coronal hole effect does not seem to be important; the overall shape outlined is fitted well with a smooth elliptical shape.

3.2. Properties of the NMC Event

While the event discussed above is a classical flux rope event that contains a magnetic cloud, the event on 22 September 1999 is an interesting non-magnetic-cloud one. The latter event shows very similar properties as for the earlier event in solar remote-sensing observations, *e.g.*, originating from close to the central meridian, post-eruption loop arcade and an elongated halo CME, thus one can expect a magnetic cloud structure. However, the magnetic cloud is not observed in the *in-situ* observations, leading to the question whether a flux rope is present in this CME or not.

Figure 4 shows the *in-situ* solar wind data of the event. The *in-situ* signal of the event started at 11:45 UT on 22 September 1999, at which a shock front (indicated by the vertical red line) appeared with apparent jump in plasma temperature, density and velocity and magnetic field intensity. The shock sheath lasted for about eight hours with elevated temperature and magnetic field until 20:00 UT (indicated by the vertical solid blue line). After 20:00 UT, the solar wind plasma temperature became abnormally low, while the magnetic

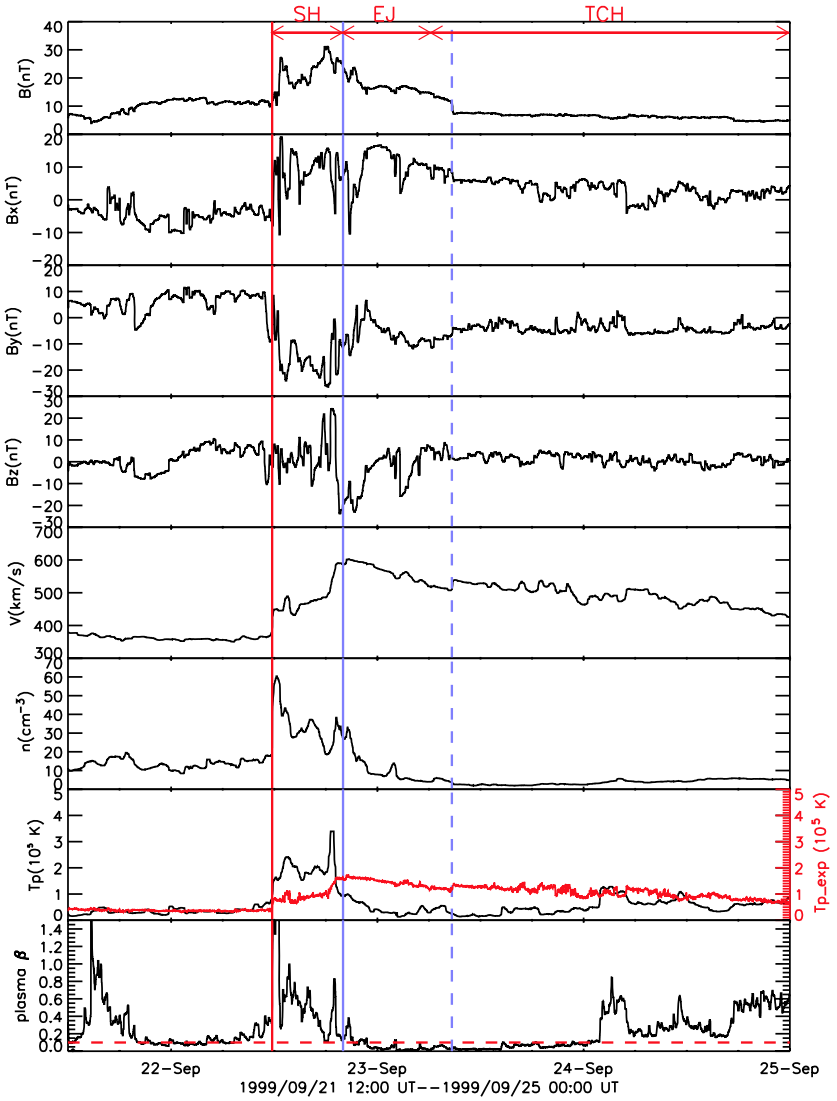

Figure 4 *In-situ* solar wind observations of the ICME event on 22 September 1999. The panels from top to bottom show, respectively, (1) solar wind magnetic field total intensity, (2) magnetic field B_x component, (3) magnetic field B_y component, (4) magnetic field B_z component, (5) solar wind plasma velocity, (6) plasma density, (6) proton temperature (black) overlaid with the expected temperature (red), and (7) the derived plasma β. The solar wind data are from the ACE spacecraft in GSE coordinates. The solid and dashed blue vertical lines indicate the starting and ending times of the ICME, which in this case is not a magnetic cloud. The vertical red line indicates the arrival time of the ICME-driven shock. The identified transient coronal hole (TCH) following the ICME or ejecta (EJ) is characterized by a long period of weak magnetic field and low plasma temperature and density.

field remained to be high until 08:40 UT on 23 September. This high-magnetic-field–low-plasma-temperature period lasted for about 13 hours, apparently corresponding to an ICME ejecta. However, this ICME ejecta did not appear as a magnetic cloud: there was no systematic rotation of the magnetic field direction. Further, the temporal profiles of the magnetic

field are rather bumpy, not as smooth as that expected from a magnetic cloud. The relatively short duration of the ejecta is also smaller than the typical size of a magnetic cloud.

Immediately following the period of the ejecta of strong magnetic field, there is a conspicuous long period of weak magnetic field, low temperature and low density that lasts for at least 39 hours, until the ending time of the display at 00:00 UT on 25 September 1999. The property of the solar wind during this period is much different from any usual transients. Neither does it correspond to a shock sheath nor ICME ejecta, since these structures usually contain a strong magnetic field. It cannot be the rear part of a corotating interaction region (CIR), albeit of weak magnetic field and low density; a typical CIR, which is believed to originate from a long-lasting low-latitude coronal hole, usually has a high plasma temperature.

What could be the solar origin of this unusual solar wind structure? We argue that it originates from a transient coronal hole (TCH) that has been forming at the footpoints of the magnetic flux rope contained in the progenitor CME. The coronal hole origin naturally explains the observed property of low plasma density and relatively weak magnetic field due to strong over-expansion of magnetic field lines, as in a usual long-lasting coronal hole. On the other hand, the low plasma temperature might be a hallmark property of a transient coronal hole, in which the ongoing cooling effect caused by the flux rope expansion still dominates the usual heating mechanism occurring in a coronal hole. Nevertheless, this argument is highly speculative, and further theoretical consideration is needed.

The existence of TCH explains why this particular ICME lacks a magnetic cloud: the *in-situ* spacecraft intercepted the leg of the flux rope instead of the nose. It is highly possible that one of the flux rope legs aligned well along the Sun–Earth line, giving rise to the long-lasting structure of weak magnetic field and low plasma temperature and density.

Since the ejecta and the TCH structures aforementioned do not appear as a magnetic cloud, we cannot fit these structures using the usual force-free flux rope model. Instead, we assume that, as a first order approximation, the structure is a simple untwisted flux tube, *i.e.*, all magnetic field lines have the same direction in the 3D space. This approximation is still valid even though the flux tube is weakly twisted. With this assumption, we can find that the overall direction of the ejecta has an inclination angle of -14° and azimuthal angle of 326° in the GSE coordinates. On the other hand, the TCH has an inclination angle of 13° and azimuthal angle of 306°. Therefore, the two structures have a very similar azimuthal angle on the equatorial plane. The inclination angles differ by about 27°, which is not surprising considering the uncertainty introduced by the averaging method.

The solar remote-sensing observations of this event support its flux rope origin (Figure 5). The progenitor CME originated from a decayed active region (panel c) located near the central meridian at W00°S23°. There appeared a large post-eruption arcade in EIT images (panels a and b). The CME was also associated with a filament eruption and a long-duration C2.8 GOES X-ray flare. The eruption produced a halo CME as seen in LASCO images (panel d). The axial orientation of the post-eruption arcade has a tilt angle with respect to the East–West direction of 31° as shown in panel b. This tilt angle is consistent with the polarity inversion line of the magnetic source region on the photospheric surface (panel c). The existence of an apparent post-eruption arcade indicates that this is an eruptive event, and the resulting CME might contain a magnetic flux rope. The axial orientation of the resulting flux rope shall follow the axis of the arcade, if the flux rope axis has not rotated during the eruption. By fitting the CME with an ellipse and further with the cone model (Figure 6), it is shown that the flux rope has a tilt angle of 10°. The difference indicates that the CME flux rope has probably rotated to have its axis more aligned with the equator than the original tilt angle at the source region. The tilt angle of the CME is highly consistent with the inclination angle of the corresponding ICME ejecta derived from *in-situ* observations.

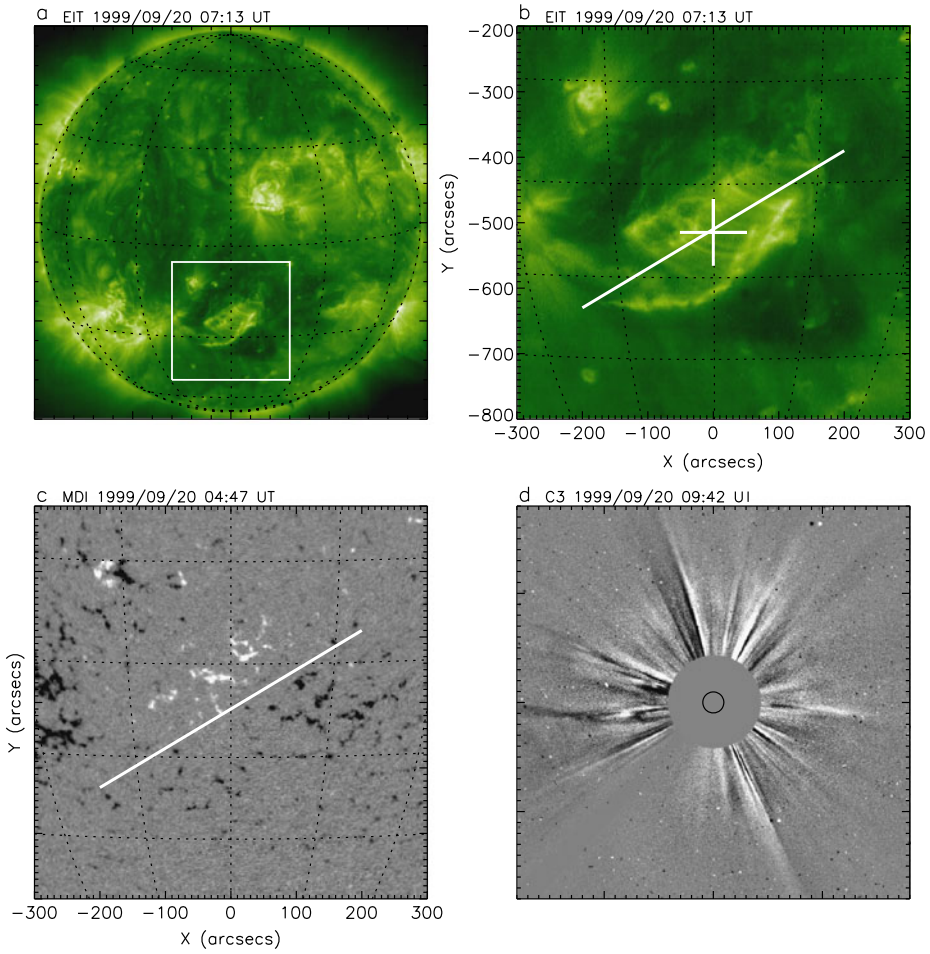

Figure 5 Solar remote-sensing observations of the source region and progenitor CME of the ICME event on 22 September 1999. (a) A full disk SOHO EIT image showing the location of the source region (inside the white square), (b) A zoom-in image of the white square area in panel (a), showing the post-eruption arcade associated with the CME. The white line indicates the orientation of the arcade, while the cross symbol indicates the location of the accompanying flare. (c) A SOHO MDI line-of-sight magnetogram image showing the photospheric magnetic field structure of the CME source region. The white line is the same as in panel (b), indicating that the orientation of the post-eruption arcade follows the polarity inversion line of the magnetic field on the surface. (d) The progenitor halo CME observed by the SOHO LASCO C2 coronagraph.

4. Discussions and Conclusion

To facilitate the discussion of the results presented above, we put together all relevant parameters of the two CME-ICME events in Table 1. The first six rows outline the timings of the Sun–Earth event chain: flare onset time, CME first-appearance time in LASCO/C2 coronagraphs, ICME-driven shock arrival time, ICME arrival time, ICME ending time, and the transient coronal hole ending time (only for the second event). The next two rows indicate the strength of the CMEs and flares, respectively. The next five rows show the geometric

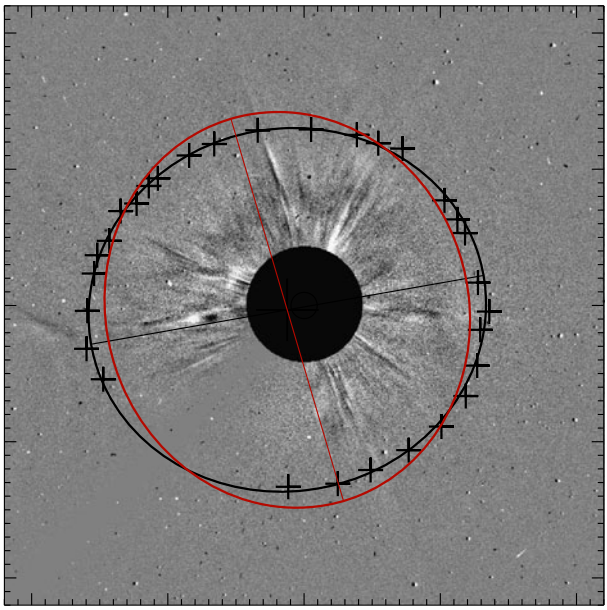

Figure 6 The geometric fitting to the observed progenitor halo CME of the ICME event on 22 September 1999. The black plus symbols are visually selected to outline the edge of the halo CME, which is fitted into an elliptic shape as indicated by the black curve; the straight black line indicates the major axis of the fitted ellipse. The ellipse shape in red line is the expected CME shape assuming a circular cone geometry of the CME, with the red straight line indicating the major axis of the ellipse. Apparently, the observed shape deviates from the circular cone model, indicating a possible flux rope structure of the CME.

parameters of the CMEs close to the Sun from remote-sensing observations, while the remaining four rows indicate the geometric parameters at 1 AU from *in-situ* observations.

Apparently, both CMEs originated from a region close to the central meridian. They also had similar appearance in coronal images with a straight post-eruption arcade and in coronagraph images with an elongated full halo shape. These similar features strongly indicate that both CMEs shall have the same magnetic structure as in their origin, very likely a magnetic flux rope. However, they differed strongly in their appearance in the near-Earth space: the first CME is a magnetic cloud, while the second is apparently not.

The question that arises from these comparative observations is why the second CME does not contain a magnetic cloud structure at 1 AU. Our answer to this question is because of the geometric selection effect at 1 AU, *i.e.*, the *in-situ* spacecraft intercepted the flank of the flux rope instead of near the nose for the second event. The conclusion of a flank interception is supported by the observation that the extended leg of the flux rope passed the near-Earth space, appearing as a TCH characterized by a long-period of weak magnetic field and low plasma temperature and density.

The cause of such a geometric effect for the central meridian CME is a non-radial propagation of the flux rope near the Sun and in the interplanetary space. One would expect that the central-meridian-originated CME should have the bulk of the flux rope or the nose pass the Earth, assuming a simple radial propagation. However, a non-radial propagation of CME is possible, depending on the magnetic field configuration in the low plasma β regime near the Sun and the relative CME-solar-wind velocity in the high plasma β regime in the interplanetary space. In the regions near the Sun, coronagraph observations have shown well that CMEs usually experience a latitudinal deflection, *e.g.*, deflected mostly from high latitude sources toward the low latitudes or equators, especially during the solar minimum (Schwenn, 2000; Gopalswamy *et al.*, 2003; Cremades, Bothmer, and Tripathi, 2006; Wang *et al.*, 2011). The non-radial longitudinal deflection, while being difficult to be directly observed in coronagraph images due to the plane-of-sky projection effect, has been inferred from comparing remote-sensing and *in-situ* observations. Such observa-

Table 1 Properties of the CME events with and without magnetic cloud.

Event	MC	NMC
Time Flare Onset (UT)	2000/10/09 23:19	1999/09/20 05:46
Time CME (UT)[a]	2000/10/09 23:50	1999/09/20 06:06
Time Shock Arrival (UT)	2000/10/12 12:42	1999/09/22 11:45
Time ICME Arrival (UT)	2000/10/13 16:20	1999/09/22 20:00
Time ICME Ending (UT)	2000/10/14 17:00	1999/09/23 08:40
Time TCH Ending (UT)[b]	NA	1999/09/25 00:00
Speed of CME (km s^{-1})	798	604
Magnitude of Flare	C6.7	C2.8
Surface Location of Flare	W14°N01°	E00°S23°
Direction of CME	W27°N27°	E24°S07°
Half Cone Angle of CME	65°	77°
INC of Eruption Arcade[c]	32°	31°
INC of CME Major Axis[c]	34°	10°
INC of ICME Axis[d]	−24°	−14°
INC of TCH Axis[d]	NA	13 °
AZI of ICME Axis[e]	140°	326°
AZI of TCH Axis[e]	NA	306°

[a]The time of the CME first appearance in LASCO C2 FOV.

[b]Approximate ending time of transient coronal hole, only for the NMC event.

[c]Inclination angle with respect to the heliospheric equator.

[d]Inclination angle with respect to the ecliptic plane as in the GSE coordinates. The angular difference between the heliospheric equator and the ecliptic plane is ignored in this study.

[e]Azimuthal angle in the GSE coordinates. Zero degree is toward the Sun, 90 degree is to the East.

tions include the apparent East–West asymmetry of solar sources of intense geomagnetic storms with more events originated in the western hemisphere (Wang *et al.*, 2002; Zhang *et al.*, 2003) and a similar asymmetry of the sources of magnetic clouds (Gopalswamy *et al.*, 2007). The longitudinal deflection can also be inferred from how individual CMEs with different source longitudes either encounter or miss the Earth (Wang *et al.*, 2006), and in particular, the identification of the unexpected "driverless" shocks at 1 AU with their solar sources close to the central meridian (Gopalswamy *et al.*, 2009). Direct evidence of longitudinal deflection was recently made possible from the measurement of the 3D trajectory of CMEs based on the twin STEREO spacecraft observations (Gui *et al.*, 2011). The research work discussed above indicates that a CME could be deflected either along the latitudinal direction or longitudinal direction.

Theoretically, a CME's trajectory can be influenced by the ambient magnetic field in the corona where a CME has to push through. It is well known that the inner corona, *e.g.*, $< \sim 3$ solar radii, is in the regime of low plasma β, *i.e.*, the magnetic force dominates plasma pressure force and other forces, and as a result, the magnetic field lines rooted in the photosphere are highly non-radial in the inner corona until they reach the heights where the momentum of solar wind flow starts to dominate the magnetic force. Thus, it is expected that in the inner corona the trajectory of the rising motion of the flux rope should be at least partially guided by the non-radial orientation of the ambient

magnetic field. It has been recognized that such magnetic deflection effect is mainly attributed to coronal holes (Cremades, Bothmer, and Tripathi, 2006; Gopalswamy *et al.*, 2009; Mohamed *et al.*, 2012), whose magnetic field is highly non-radial and also comparable in size to that of flux ropes. This kind of deflection has been empirically quantified by the so-called coronal hole influence parameter (CHIP), whose magnitude for each coronal hole depends on the distance between the coronal hole centroid and the eruption area, the coronal hole area and the average magnetic field at the photospheric level (Gopalswamy *et al.*, 2009; Mohamed *et al.*, 2012). Recently, Shen *et al.* (2011) proposed a more general parameter, the magnetic energy density parameter that includes the contributions from all fields instead of only that from coronal holes; in this model, the flux rope is deflected toward the region of minimum coronal magnetic energy density.

Far from the inner corona, STEREO observations have also provided evidence that a CME may deflect or deviate from the radial direction in the interplanetary space (Lugaz *et al.*, 2010). The deflection is probably caused by the Parker spiral magnetic field embedded in the radially flowing solar wind (Wang *et al.*, 2004). A CME traveling faster than the ambient solar wind is expected to deflect toward the East, due to the piling-up of the interplanetary magnetic field in front of the CME; Such enhanced magnetic field has a force component pointing toward the East along the transverse direction. On the other hand, a slow CME is expected to be deflected toward the West. Nevertheless, since the magnetic field in the interplanetary space is weak and the plasma is in the regime of high β, the rate of deflection in the interplanetary space should be smaller than that in the inner corona.

In summary, we have studied two carefully chosen CME events, both of which originated close to the central meridian and showed similar properties near the Sun in remote-sensing observations. We argue that the difference in the *in-situ* observations, *i.e.*, a magnetic cloud appearing in the first event but not in the second event, is caused by the geometric selection effect. The first event had its nose pass through the observing spacecraft, thus the intrinsic flux rope structure of the CME appeared as a magnetic cloud. On the other hand, the second event had the flank of the flux rope intercept the spacecraft, thus did not appear as a magnetic cloud. We further argue that a conspicuous long period of weak magnetic field, low plasma temperature and density in the second event should correspond to the extended leg portion of the embedded magnetic flux rope in the interplanetary space, thus validating the scenario of flank-passing. These observations support the idea that all CMEs arriving at the Earth include flux ropes.

Acknowledgements We acknowledge the support from NSF ATM-0748003 and NSF AGS-1156120. The ACE plasma, magnetic field, and composition/charge state data were provided by the ACE Science Center. SOHO is a project of international cooperation between ESA and NASA. The LASCO instrument was constructed by a consortium of the Naval Research Laboratory, University of Birmingham (England), the Max-Planck-Institute für Aeronomie (Germany) and the Laboratoire d'Astronomie Spatiale (France).

References

Amari, T., Luciani, J.F., Aly, J.J., Mikic, Z., Linker, J.: 2003, Coronal mass ejection: initiation, magnetic helicity, and flux ropes. I. Boundary motion-driven evolution. *Astrophys. J.* **585**, 1073. doi:10.1086/345501.

Antiochos, S.K., DeVore, C.R., Klimchuk, J.A.: 1999, A model for solar coronal mass ejections. *Astrophys. J.* **510**, 485. doi:10.1086/306563.

Aulanier, G., Török, T., Démoulin, P., DeLuca, E.E.: 2010, Formation of torus-unstable flux ropes and electric currents in erupting sigmoids. *Astrophys. J.* **708**, 314. doi:10.1088/0004-637X/708/1/314.

Bothmer, V., Schwenn, R.: 1996, Signatures of fast CMEs in interplanetary space. *Adv. Space Res.* **17**, 319.

Burlaga, L., Sittler, E., Mariani, F., Schwenn, R.: 1981, Magnetic loop behind an interplanetary shock: Voyager, Helios, and IMP 8 observations. *J. Geophys. Res.* **86(A8)**, 6673.

Canfield, R.C., Hudson, H.S., McKenzie, D.E.: 1999, Sigmoidal morphology and eruptive solar activity. *Geophys. Res. Lett.* **26**, 627. doi:10.1029/1999GL900105.

Chen, J.: 1996, Theory of prominence eruption and propagation: interplanetary consequences. *J. Geophys. Res.* **101**, 27499. doi:10.1029/96JA02644.

Cheng, X., Zhang, J., Liu, Y., Ding, M.D.: 2011, Observing flux rope formation during the impulsive phase of a solar eruption. *Astrophys. J. Lett.* **732**, L25. doi:10.1088/2041-8205/732/2/L25.

Cremades, H., Bothmer, V., Tripathi, D.: 2006, Properties of structured coronal mass ejections in solar cycle 23. *Adv. Space Res.* **38**, 461. doi:10.1016/j.asr.2005.01.095.

Dere, K.P., Brueckner, G.E., Howard, R.A., Michels, D.J., Delaboudinière, J.P.: 1999, LASCO and EIT observations of helical structure in coronal mass ejections. *Astrophys. J.* **516**, 465. doi:10.1086/307101.

Fan, Y., Gibson, S.E.: 2007, Onset of coronal mass ejections due to loss of confinement of coronal flux ropes. *Astrophys. J.* **668**, 1232. doi:10.1086/521335.

Gibson, S.E., Fletcher, L., Del Zanna, G., Pike, C.D., Mason, H.E., Mandrini, C.H., Démoulin, P., Gilbert, H., Burkepile, J., Holzer, T., Alexander, D., Liu, Y., Nitta, N., Qiu, J., Schmieder, B., Thompson, B.J.: 2002, The structure and evolution of a sigmoidal active region. *Astrophys. J.* **574**, 1021. doi:10.1086/341090.

Gopalswamy, N., Yashiro, S., Kaiser, M.L., Howard, R.A., Bougeret, J.L.: 2001, Radio signatures of coronal mass ejection interaction: coronal mass ejection cannibalism? *Astrophys. J. Lett.* **548**, L91.

Gopalswamy, N., Shimojo, M., Lu, W., Yashiro, S., Shibasaki, K., Howard, R.A.: 2003, Prominence eruptions and coronal mass ejection: a statistical study using microwave observations. *Astrophys. J.* **586**, 562. doi:10.1086/367614.

Gopalswamy, N., Akiyama, S., Yashiro, S., Michalek, G., Lepping, R.P.: 2007, Solar sources and geospace consequences of interplanetary magnetic clouds observed during solar cycle 23. *J. Atmos. Solar-Terr. Phys.* doi:10.1016/j.jastp.2007.08.070.

Gopalswamy, N., Mäkelä, P., Xie, H., Akiyama, S., Yashiro, S.: 2009, CME interactions with coronal holes and their interplanetary consequences. *J. Geophys. Res.* **114**. doi:10.1029/2008JA013686.

Gosling, J.T.: 1990, Coronal mass ejections and magnetic flux ropes in interplanetary space. In: Russell, C.T., Priest, E.R., Lee, L.C. (eds.) *Physics of Magnetic Flux Ropes*, *Geophys. Monogr. Ser.* **58**, AGU, Washington, 343.

Gosling, J.T., McComas, D.J., Phillips, J.L., Bame, S.J.: 1991, Geomagnetic activity associated with Earth passage of interplanetary shock disturbances and coronal mass ejections. *J. Geophys. Res.* **96**, 7831.

Green, L.M., Kliem, B.: 2009, Flux rope formation preceding coronal mass ejection onset. *Astrophys. J. Lett.* **700**, L83. doi:10.1088/0004-637X/700/2/L83.

Gui, B., Shen, C., Wang, Y., Ye, P., Liu, J., Wang, S., Zhao, X.: 2011, Quantitative analysis of CME deflections in the corona. *Solar Phys.* **271**, 111. doi:10.1007/s11207-011-9791-9.

Henke, T., Woch, J., Schwenn, R., Mall, U., Gloeckler, G., von Steiger, R., Forsyth, R.J., Balogh, A.: 2001, Ionization state and magnetic topology of coronal mass ejections. *J. Geophys. Res.* **106**, 10597. doi:10.1029/2000JA900176.

Kliem, B., Török, T.: 2006, Torus instability. *Phys. Rev. Lett.* **96**, 255002. doi:10.1103/PhysRevLett.96.255002.

Lepping, R.P., Jones, J.A., Burlaga, L.F.: 1990, Magnetic field structure of interplanetary magnetic clouds at 1 AU. *J. Geophys. Res.* **95**, 11957.

Liu, R., Liu, C., Wang, S., Deng, N., Wang, H.: 2010, Sigmoid-to-flux-rope transition leading to a loop-like coronal mass ejection. *Astrophys. J. Lett.* **725**, L84. doi:10.1088/2041-8205/725/1/L84.

Lugaz, N., Hernandez-Charpak, J.N., Roussev, I.I., Davis, C.J., Vourlidas, A., Davies, J.A.: 2010, Determining the azimuthal properties of coronal mass ejections from multi-spacecraft remote-sensing observations with STEREO SECCHI. *Astrophys. J.* **715**, 493. doi:10.1088/0004-637X/715/1/493.

McKenzie, D.E., Canfield, R.C.: 2008, Hinode XRT observations of a long-lasting coronal sigmoid. *Astron. Astrophys.* **481**, L65. doi:10.1051/0004-6361:20079035.

Mohamed, A.A., Gopalswamy, N., Yashiro, S., Akiyama, S., Mäkelä, P., Xie, H., Jung, H.: 2012, The relation between coronal holes and coronal mass ejections during the rise, maximum, and declining phases of solar cycle 23. *J. Geophys. Res.* **117**(A16), 1103. doi:10.1029/2011JA016589.

Moore, R.L., Sterling, A.C., Hudson, H.S., Lemen, J.R.: 2001, Onset of the magnetic explosion in solar flares and coronal mass ejections. *Astrophys. J.* **552**, 833. doi:10.1086/320559.

Olmedo, O., Zhang, J.: 2010, Partial torus instability. *Astrophys. J.* **718**, 433. doi:10.1088/0004-637X/718/1/433.

Richardson, I.G., Cane, H.V.: 1995, Regions of abnormally low proton temperature in the solar wind (1965 – 1991) and their association with ejecta. *J. Geophys. Res.* **100**, 23397. doi:10.1029/95JA02684.

Richardson, I.G., Cane, H.V.: 2004, The fraction of interplanetary coronal mass ejections that are magnetic clouds: evidence for a solar cycle variation. *Geophys. Res. Lett.* **31**, L18804.
Riley, P., Crooker, N.U.: 2004, Kinematic treatment of coronal mass ejection evolution in the solar wind. *Astrophys. J.* **600**, 1035. doi:10.1086/379974.
Rust, D.M.: 1994, Spawning and shedding helical magnetic fields in the solar atmosphere. *Geophys. Res. Lett.* **21**, 241.
Schrijver, C.J.: 2009, Driving major solar flares and eruptions: a review. *Adv. Space Res.* **43**, 739. doi:10.1016/j.asr.2008.11.004.
Schwenn, R.: 2000, Heliospheric 3d structure and CME propagation as seen from SOHO: recent lessons for space weather predictions. *Adv. Space Res.* **26**, 43. doi:10.1016/S0273-1177(99)01025-X.
Shen, C., Wang, Y., Gui, B., Ye, P., Wang, S.: 2011, Kinematic evolution of a slow CME in corona viewed by STEREO-B on 8 October 2007. *Solar Phys.* **269**, 389. doi:10.1007/s11207-011-9715-8.
Sterling, A.C., Hudson, H.S.: 1997, YOHKOH SXT observations of X-ray "dimming" associated with a halo coronal mass ejection. *Astrophys. J. Lett.* **491**, L55.
Titov, V.S., Démoulin, P.: 1999, Basic topology of twisted magnetic configurations in solar flares. *Astron. Astrophys.* **351**, 707.
Tripathi, D., Kliem, B., Mason, H.E., Young, P.R., Green, L.M.: 2009, Temperature tomography of a coronal sigmoid supporting the gradual formation of a flux rope. *Astrophys. J. Lett.* **698**, L27. doi:10.1088/0004-637X/698/1/L27.
Vourlidas, A., Wu, S.T., Wang, A.H., Subramanian, P., Howard, R.A.: 2003, Direct detection of a coronal mass ejection-associated shock in large angle and spectrometric coronagraph experiment white-light images. *Astrophys. J.* **598**, 1392. doi:10.1086/379098.
Wang, Y.M., Ye, P.Z., Wang, S., Zhou, G.P., Wang, J.X.: 2002, A statistical study on the geoeffectiveness of Earth-directed coronal mass ejections from March 1997 to December 2000. *J. Geophys. Res.* **107**, 1340. doi:10.1029/2002JA009244.
Wang, Y.M., Ye, P.Z., Wang, S., Xue, X.H.: 2003, An interplanetary cause of large geomagnetic storms: fast forward shock overtaking preceding magnetic cloud. *Geophys. Res. Lett.* **30**, 1700. doi:10.1029/2002GL016861.
Wang, Y., Shen, C., Ye, P., Wang, S.: 2004, Deflection of coronal mass ejection in the interplanetary medium. *Solar Phys.* **222**, 329.
Wang, Y., Xue, X., Shen, C., Ye, P., Wang, S., Zhang, J.: 2006, Impact of major coronal mass ejections on geospace during 2005 September 7 – 13. *Astrophys. J.* **646**, 625. doi:10.1086/504676.
Wang, Y., Chen, C., Gui, B., Shen, C., Ye, P., Wang, S.: 2011, Statistical study of coronal mass ejection source locations: understanding CMEs viewed in coronagraphs. *J. Geophys. Res.* **116**, 4104. doi:10.1029/2010JA016101.
Wood, B.E., Howard, R.A.: 2009, An empirical reconstruction of the 2008 April 26 coronal mass ejection. *Astrophys. J.* **702**, 901. doi:10.1088/0004-637X/702/2/901.
Wood, B.E., Wu, C.-C., Rouillard, A.P., Howard, R.A., Socker, D.G.: 2012, A coronal hole's effects on coronal mass ejection shock morphology in the inner heliosphere. *Astrophys. J.* **755**, 43. doi:10.1088/0004-637X/755/1/43.
Xie, H., Ofman, L., Lawrence, G.: 2004, Cone model for halo CMEs: application to space weather forecasting. *J. Geophys. Res.* **109**, A03109.
Zhang, J., Cheng, X., Ding, M.-D.: 2012, Observation of an evolving magnetic flux rope before and during a solar eruption. *Nat. Commun.* **3**, 747. doi:10.1038/ncomms1753.
Zhang, J., Dere, K.P., Howard, R.A., Kundu, M.R., White, S.M.: 2001, On the temporal relationship between coronal mass ejections and flares. *Astrophys. J.* **559**, 452. doi:10.1086/322405.
Zhang, J., Dere, K.P., Howard, R.A., Bothmer, V.: 2003, Identification of solar sources of major geomagnetic storms between 1996 and 2000. *Astrophys. J.* **582**, 520.
Zhang, J., Richardson, I.G., Webb, D.F., Gopalswamy, N., Huttunen, E., Kasper, J.C., Nitta, N.V., Poomvises, W., Thompson, B.J., Wu, C.-C., Yashiro, S., Zhukov, A.N.: 2007, Solar and interplanetary sources of major geomagnetic storms (Dst ≤ -100 nT) during 1996 – 2005. *J. Geophys. Res.* **112**, 10102. doi:10.1029/2007JA012321.
Zhao, X.P., Plunkett, S.P., Liu, W.: 2002, Determination of geometrical and kinematical properties of halo coronal mass ejections using the cone model. *J. Geophys. Res.* **107**, 1223. doi:10.1029/2001JA009143.
Zurbuchen, T.H., Richardson, I.G.: 2006, *In-situ* solar wind and magnetic field signatures of interplanetary coronal mass ejections. *Space Sci. Rev.* **123**, 31. doi:10.1007/s11214-006-9010-4.